This article was downloaded by: [Institute Of Atmospheric Physics]
On: 09 December 2014, At: 15:15
Publisher: Taylor & Francis
Informa Ltd Registered in England and Wales Registered Number: 1072954 Registered office: Mortimer House, 37-41 Mortimer Street, London W1T 3JH, UK

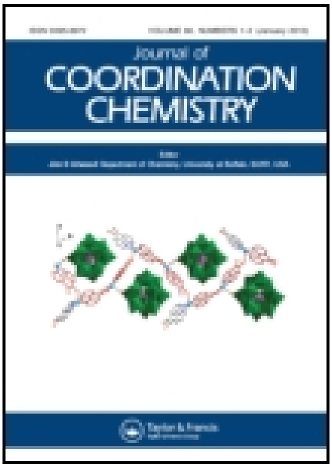

Click for updates

Journal of Coordination Chemistry
Publication details, including instructions for authors and subscription information:
http://www.tandfonline.com/loi/gcoo20

Energetic materials composed of coordination polymers: $\{[Zn(\mu\text{-atrz})_3](ClO_4)_2\cdot 2H_2O\}_n$ and $\{[Cu(\mu\text{-atrz})_3](NO_3)_2\cdot 2H_2O\}_n$

Y.L. Li[a], B.D. Wu[a], H. Qiu[a], T.L. Zhang[a] & L. Yang[a]
[a] State Key Laboratory of Explosion Science and Technology, Beijing Institute of Technology, Beijing, China

Accepted author version posted online: 02 Jul 2014.Published online: 14 Jul 2014.

To cite this article: Y.L. Li, B.D. Wu, H. Qiu, T.L. Zhang & L. Yang (2014) Energetic materials composed of coordination polymers: $\{[Zn(\mu\text{-atrz})_3](ClO_4)_2\cdot 2H_2O\}_n$ and $\{[Cu(\mu\text{-atrz})_3](NO_3)_2\cdot 2H_2O\}_n$, Journal of Coordination Chemistry, 67:11, 2016-2027, DOI: 10.1080/00958972.2014.935770

To link to this article: http://dx.doi.org/10.1080/00958972.2014.935770

PLEASE SCROLL DOWN FOR ARTICLE

Taylor & Francis makes every effort to ensure the accuracy of all the information (the “Content”) contained in the publications on our platform. However, Taylor & Francis, our agents, and our licensors make no representations or warranties whatsoever as to the accuracy, completeness, or suitability for any purpose of the Content. Any opinions and views expressed in this publication are the opinions and views of the authors, and are not the views of or endorsed by Taylor & Francis. The accuracy of the Content should not be relied upon and should be independently verified with primary sources of information. Taylor and Francis shall not be liable for any losses, actions, claims, proceedings, demands, costs, expenses, damages, and other liabilities whatsoever or howsoever caused arising directly or indirectly in connection with, in relation to or arising out of the use of the Content.

This article may be used for research, teaching, and private study purposes. Any substantial or systematic reproduction, redistribution, reselling, loan, sub-licensing, systematic supply, or distribution in any form to anyone is expressly forbidden. Terms &

Journal of Coordination Chemistry, 2014
Vol. 67, No. 11, 2016–2027, http://dx.doi.org/10.1080/00958972.2014.935770

Energetic materials composed of coordination polymers: $\{[Zn(\mu\text{-atrz})_3](ClO_4)_2{\cdot}2H_2O\}_n$ and $\{[Cu(\mu\text{-atrz})_3](NO_3)_2{\cdot}2H_2O\}_n$

Y.L. LI, B.D. WU, H. QIU, T.L. ZHANG and L. YANG*

State Key Laboratory of Explosion Science and Technology, Beijing Institute of Technology, Beijing, China

(*Received 24 October 2013; accepted 31 March 2014*)

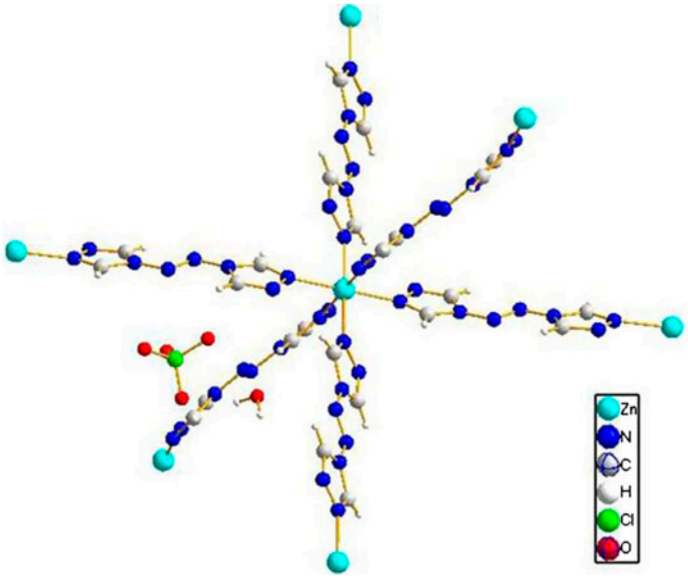

An improved synthetic pathway for *trans*-4,4′-azo-1,2,4-triazole (atrz) was discovered. Pure atrz was obtained directly without any other separation step in an environment friendly process. Treatment of atrz with zinc perchlorate and cupric nitrate led to the isolation of $\{[Zn(\mu\text{-atrz})_3](ClO_4)_2{\cdot}2H_2O\}_n$ and $\{[Cu(\mu\text{-atrz})_3](NO_3)_2{\cdot}2H_2O\}_n$, which were well characterized. Their structures were determined by X-ray crystallographic analysis. The calculation results of the formation of $\{[Zn(\mu\text{-atrz})_3](ClO_4)_2\ 2H_2O\}_n$ and $\{[Cu(\mu\text{-atrz})_3](NO_3)_2\ 2H_2O\}_n$ indicates that the perfect crystal structures in spite of much resistance. A fundamental understanding of the structure and thermal properties involves factors, such as conjugated system, crystal structure, and inorganic metallic compounds that affect their thermal behavior. The high energy of the coordination compounds consists of chemical, electronic, and potential energy. The potential for the improvement of the coordination polymer opens up a new world for research of energetic materials.

Keywords: Improved pathway; $\{[Zn(\mu\text{-atrz})_3](ClO_4)_2{\cdot}2H_2O\}_n$; $\{[Cu(\mu\text{-atrz})_3](NO_3)_2{\cdot}2H_2O\}_n$; Perfect crystal structure; Theoretical research; Thermal properties; The great potential for improvement

---

*Corresponding author. Email: yanglibit@bit.edu.cn

1. Introduction

C–N heteroaromatic compounds with high-nitrogen content [1, 2] have attracted significant attention from many researchers because of their high-energy density [3, 4], high positive heat of formation (+ΔH_f) [5–7], and high thermal stability [8–10] that result in numerous applications including solid fuels in micropropulsion systems [11, 12], gas generators [13], and smoke-free pyrotechnic fuels [14, 15]. This tradition has led to many advances on energetic materials in the unimolecule chemistry field. Hiskey [16–19] has done some great research on tetrazine and tetrazole including 3,6-diazido-1,2,4,5-tetrazine (DiAT), energetic salts of the 5,5′-azotetrazolate anion with different guandinium cations, etc. Klapötke [20–24] got a 1,1′-azobis(tetrazole) (N_{10} compound), 1,5-diamino-4-methyltetrazolium dinitramide, anionic tetrazole-2N-oxide, and some other energetic compounds. Shreeve [25, 26] synthesized various new polynitro-1,2,4-triazoles containing a trinitromethyl group and their salts in 2011. Meanwhile, Pang [27–31] reported the synthesis of 1,1′-azobis-1,2,3-triazole (N_8 compound), and polyazido- and polyamino-substituted N,N′-azo-1,2,4-triazole. These give us models to design new supramolecular energetic materials.

Trans-4,4′-azo-1,2,4-triazole (atrz) is an ideal ligand because of its strong coordination ability (figure 1. The negative electrostatic potential concentrates on both molecular bare ends.), simple molecular structure, potential for improvement [30–32], and high thermal stability [29]. In 2007, Li [28] first prepared atrz using sodium dichloroisocyanurate as the oxidative reagent, but there were still unsolved problems. First, the atom utilization of sodium dichloroisocyanurate was very low since only chlorine was used. It was difficult to get pure atrz as a result of residues left. Second, the needle-like sample (Supplemental data, figure S2, see online at http://dx.doi.org/10.1080/00958972.2014.935770), which was very dangerous, was obtained when we used the method of Sheng-Hua Li to synthesize atrz. As part of our continual effort in high-nitrogen energetic materials, we herein report an improved synthetic pathway for atrz.

In 2012, Liu [33] and Chuang [34] reported the synthesis of a 1-D coordination polymer (CP) $[Co(SCN)_2(bta)(H_2O)_2]$ and CPs of iron(II) with the formula $[Fe(\mu\text{-atrz})_3]X_2{\cdot}2H_2O$ (where $X = ClO_4^-$ and BF_4^-) in a 3-D framework and $[Fe(\mu\text{-atrz})(\mu\text{-pyz})(NCS)_2]{\cdot}4H_2O$ ($3{\cdot}4H_2O$) in a 2-D layer structure using atrz as ligand; their research just concentrated on magnetic properties of these CPs. Research in the field of energetic material of CPs was almost blank. Therefore, we report here two new members of CPs with the formula $\{[Zn(\mu\text{-atrz})_3](ClO_4)_2{\cdot}2H_2O\}_n$ and $\{[Cu(\mu\text{-atrz})_3](NO_3)_2{\cdot}2H_2O\}_n$ in an ideal crystal structure. The thermal properties and structure are investigated. A fundamental understanding of the structure and thermal properties elucidates the factors, such as conjugated system and crystal structure that affect the thermal behavior.

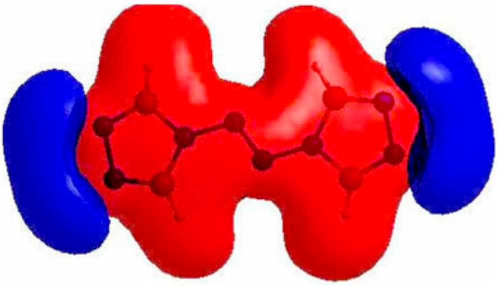

Figure 1. Molecular electrostatic potential surface of atrz. Blue : negative, red : positive (see http://dx.doi.org/10.1080/00958972.2014.935770 for color version).

2. Experimental

2.1. *Materials and methods*

All chemicals of reagent grade were purchased and used without purification. Available chlorine content of the purchased sodium hypochlorite solution is 10%. Infrared spectra (IR) of the solid samples diluted with KBr were measured with a Bruker Equinox-55 FT-IR instrument. Elemental analyses were carried out using a 560PE-2400(II) instrument. The thermal behaviors of atrz, $\{[Zn(\mu\text{-atrz})_3](ClO_4)_2{\cdot}2H_2O\}_n$, and $\{[Cu(\mu\text{-atrz})_3](NO_3)_2{\cdot}2H_2O\}_n$ were respectively measured using a Pyris-1 differential scanning calorimeter (Perkin Elmer, USA) with a heating rate of 5 °C min^{-1} using dry oxygen-free nitrogen from 0 to 600 °C. According to the method of flame sensitivity test, impact sensitivity was determined by Fall Hammer Apparatus. Fifty milligram of sample was placed between two steel poles and then was hit by 5 kg drop hammer at different heights. Friction sensitivity was determined using 20 mg sample, when the sample was compressed between two steel poles with smooth surface at a pressure of 1.96 MPa and then was horizontally hit by 1.5 kg drop hammer from 90°.

2.2. *Synthesis of trans-4,4′-azo-1,2,4-triazole*

12.78 grams of sodium hypochlorite solution (36 mM available chlorine) was dissolved in the solution formed by mixing 5 mL glacial acetic acid with 30 mL of deionized water and the solution was cooled to 7 °C. To this was added 1.5 g (18 mM) 4-amino-1,2,4-triazole dissolved in 15 mL deionized water. The solution was stirred at 7 °C for 4 h followed by standing the final solution two days at room temperature. Yellow and oblong crystal of atrz (Supplemental data, figure S1) was obtained in 75% yield (scheme 1). This is very good for the synthesis of atrz, because the separation of the product, we know, always is the most difficult step during the whole synthetic experiment. In addition, sodium chloride, totally environment friendly, will only be left after atrz is separated from the final solution. *Caution*: The light, which makes sodium hypochlorite turn into sodium chloride and oxygen, must be obstructed during the whole reaction. Temperature is also very important to the yield of atrz because sodium hypochlorite is very unstable at high temperature (>25 °C). Anal. Calcd for $C_4N_8H_4$: C, 29.24; N, 68.32; H, 2.44. Found: C, 28.93; N, 68.36; H, 2.49. IR(cm^{-1}) = 3111(s), 1489(s), 1368(s), 1315(m), 1176(s).

2.3. *Synthesis of trans$\{[Zn(\mu\text{-atrz})_3](ClO_4)_2\ 2H_2O\}_n$ and $\{[Cu(\mu\text{-atrz})_3](NO_3)_2\ 2H_2O\}_n$*

About 1.5 mM (0.246 g) atrz was dissolved in 20 mL deionized water and the solution heated to 80 °C. To this was added the solution formed by mixing 0.5 mM $Zn(ClO_4)_2$ or $Cu(NO_3)_2$ with 20 mL deionized water drop by drop. The solution was stirred at 80 °C for 0.5 h and filtered at 40 °C. Yellow single crystals of $\{[Zn(\mu\text{-atrz})_3](ClO_4)_2{\cdot}2H_2O\}_n$ and blue single crystals of $\{[Cu(\mu\text{-atrz})_3](NO_3)_2{\cdot}2H_2O\}_n$ were obtained by slow evaporation of the final solution at room temperature within several days. Anal. Calcd for $C_{12}H_{16}C_{l2}N_{24}O_{10}Zn$: C,

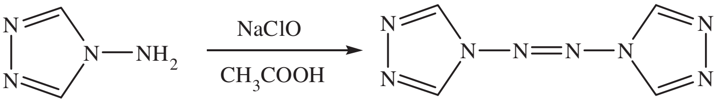

Scheme 1. Synthesis of atrz.

18.16; N, 42.38; H, 2.02. Found: C, 18.02; N, 42.27; H, 2.06. IR(cm^{-1}) = 3119(s), 1502(s), 1392(s), 1317(m), 1187(s). Anal. Calcd for $C_{12}H_{16}N_{26}O_8Cu$: C, 20.11; N, 50.83; H, 2.23. Found: C, 18.06; N, 50.71; H, 2.26. IR(cm^{-1}) = 3119(s), 1502(s), 1392(s), 1317(m), 1187(s).

2.4. *X-ray single crystal structure determination*

Diffraction data of atrz, $\{[Zn(\mu\text{-atrz})_3](ClO_4)_2\cdot 2H_2O\}_n$, and $\{[Cu(\mu\text{-atrz})_3](NO_3)_2\cdot 2H_2O\}_n$ were collected on a Rigaku AFC-10/Saturn 724^+ CCD diffractometer with graphite-monochromated Mo Kα radiation ($\lambda = 0.071073$ nm) at 93(2) K with a multi-scan mode. The structure was solved using SHELXS-97 [35] program, refined by full-matrix least-squares on F^2 with SHELXL-97 [36] and finally checked with PLATON software. All non-hydrogen atoms were obtained from the difference Fourier map and refined anisotropically. The hydrogens were obtained geometrically and treated by a constrained refinement (results shown in table 1).

2.5. *Theoretical research*

Natural bond orbital (NBO) analysis of atrz was carried out using the Gaussian 03 program package [37] and B3LYP/6-311G method. The calculation of statistical thermodynamics enthalpy of $\{[Zn(\mu\text{-atrz})_3](ClO_4)_2\cdot 2H_2O\}_n$ and $\{[Cu(\mu\text{-atrz})_3](NO_3)_2\cdot 2H_2O\}_n$ was performed using the Dmol [37] package [38, 39] in Materials Studio 5.0 based on DFT(PW91 [40]) and double numerical plus d-functions (DND) basis considering the complexity of the studied system containing almost 130 atoms, shown in figure 2. ECP [41, 42] (the effective core potentials) method was employed on the kernel electronics of Zn^{2+} and Cu^{2+} to simplify the calculation (replacing the kernel electronics with the single effective potential). Spin restrictive method was adopted to optimize the geometry structure of $\{[Zn(\mu\text{-atrz})_3](ClO_4)_2\cdot 2H_2O\}_n$, because the central zinc(II) has no single electron, but spin unrestrictive method was used for $\{[Cu(\mu\text{-atrz})_3](NO_3)_2\cdot 2H_2O\}_n$, because of a single electron of copper (II). The convergence criterion of the self-consistent field iterative computations for the energy and electron density of the system are respectively 2.0×10^{-5} a.u. and 1.0×10^{-5} a.u. Brillouin zone sampling was performed using the Monkhorst–Pack scheme with a *k*-point grid of 5 × 2 × 5. These values were determined to ensure the convergence of total energies.

Table 1. Crystallographic details.

Compound	Atrz	$\{[Zn(4,4'\text{-ATZ})_3](ClO_4)_2\cdot 2H_2O\}_n$	$\{[Cu(\mu\text{-atrz})_3](NO_3)_2\cdot 2H_2O\}_n$
Formula	$C_2H_2N_4$	$C_{12}H_{16}Cl_2N_{24}O_{10}Zn$	$C_{12}H_{16}N_{26}O_8Cu$
Formula weight (g M^{-1})	82.08	792.76	716.05
Temperature (K)	153(2)	143(2)	153(2)
Crystal system	Monoclinic	Monoclinic	Monoclinic
Space group	*P2(1)/n*	*P2(1)/n*	*P2(1)/n*
a (Å)	4.975(2)	8.130(2)	8.0203(19)
b (Å)	6.470(3)	20.174(5)	20.455(5)
c (Å)	10.210(5)	9.014(2)	8.612(2)
α (°)	90	90	90
β (°)	92.125(7)	91.423(4)	90.650(4)
γ (°)	90	90	90
Volume (Å^3)	328.4(3)	1478.0(6)	1412.8(6)
Z	4	2	2
Density Calcd (g cm^{-3})	1.660	1.781	1.683
R_1/wR_2 (all data)	0.0438/0.0940	0.0597/0.1187	0.0640/0.1398
R_1/wR_2 ($I > 2\sigma(I)$)	0.0370/0.0892	0.0496/0.1120	0.0519/0.1238
CCDC		930556	956282

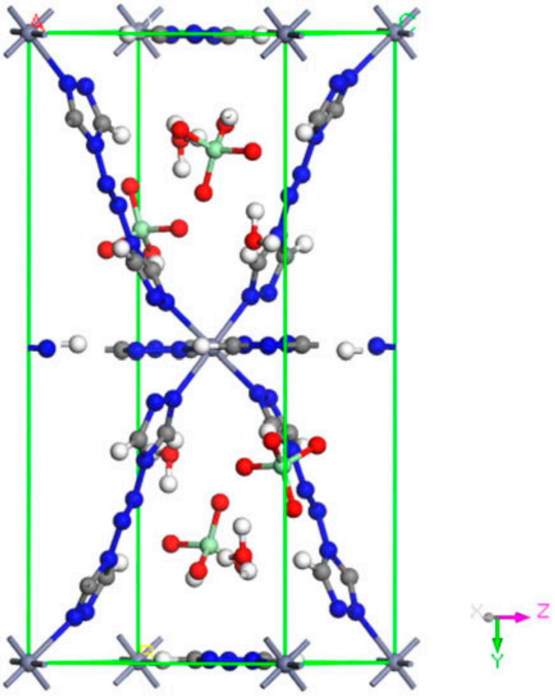

Figure 2. The studied system in MS.

3. Results and discussion

3.1. *Description of the structures of atrz*

Atrz crystallizes in the monoclinic space group *P2(1)/n* with two formula units in the unit cell and a density of 1.660 g cm^{-3}. The structure of atrz about the azo double bond is *trans*, and the azo double bond is 1.248 Å long, shorter than that in the N_8 compound [27] at 1.250 Å, but longer than that in the N_{10} compound [20] at 1.178 Å. NBO analysis of atrz is fully credible according to the structure parameters shown in table 2. Negative charge concentrates on N_1 and N_8 that are symmetrical as shown in table S1 and figure S3 in Supplemental data. The degeneration of HOMO-1 and HOMO orbitals is shown as figure 3. A large conjugated system exists in the molecule.

3.2. *Description of the structures of $\{[Zn(\mu\text{-}atrz)_3](ClO_4)_2\cdot 2H_2O\}_n$ and $\{[Cu(\mu\text{-}atrz)_3](NO_3)_2\cdot 2H_2O\}_n$*

$\{[Zn(\mu\text{-atrz})_3](ClO_4)_2\cdot 2H_2O\}_n$ crystallizes in the monoclinic space group *P2(1)/n* with a density of 1.781 g cm^{-3} that is bigger than that of a 2-D polymeric Ca(II) compound with tetrazole-1-acetic acid by Li [43]. As shown in figure 4, the zinc(II) is coordinated by six μ-atrz ligands in a nearly regular ZnN_6 octahedron that also can be proved by the bond angles

Table 2. Selected bond lengths (Å) and angles (°) of atrz, $\{[Zn(\mu\text{-atrz})_3](ClO_4)_2{\cdot}2H_2O\}_n$ and $\{[Cu(\mu\text{-atrz})_3](NO_3)_2{\cdot}2H_2O\}_n$.

	B3LYP	Expt		B3LYP	Expt
Atrz					
N_3–N_{10}	1.248	1.248	N_2–N_3–N_{10}	110.4	110.5
N_3–N_2	1.380	1.380	N_3–N_2–C_4	121.4	122.4
N_2–C_4	1.368	1.367	N_2–C_4–N_1	108.8	125.0
N_2–C_6	1.374	1.374	C_4–N_1–N_{16}	107.2	107.0
N_1–C_4	1.304	1.303	N_1–N_{16}–C_6	108.3	107.7
N_{16}–N_1	1.412	1.412	N_{16}–C_6–N_2	108.8	109.4
$\{[Zn(\mu\text{-atrz})_3](ClO_4)_2{\cdot}2H_2O\}_n$					
Zn_1–N_9	2.154	Zn_1–N_1	2.161	Zn_1–N_{7B}	2.153
N_{12}–N_{12D}	1.244	N_4–N_5	1.242	N_{4B}–N_{5B}	1.242
N_{11}–N_{12}	1.380	N_3–N_4	1.387	N_{3B}–N_{4B}	1.387
N_{11D}–N_{12D}	1.380	N_5–N_6	1.388	N_{5B}–N_{6B}	1.388
N_9–N_{10}	1.398	N_1–N_2	1.400	N_{7B}–N_{8B}	1.394
N_{9D}–N_{10D}	1.398	N_7–N_8	1.394	N_{1B}–N_{2B}	1.400
$\{[Cu(\mu\text{-atrz})_3](NO_3)_2{\cdot}2H_2O\}_n$					
Cu_1–N_9	2.028	Cu_1–N_1	2.377	Cu_1–N_5	2.010
N_{12}–N_{8E}	1.242	N_4–N_{4E}	1.227	N_8–N_{12B}	1.227
N_{11}–N_{12}	1.378	N_3–N_4	1.393	N_7–N_8	1.393
N_{7E}–N_{8E}	1.378	N_{3E}–N_{4E}	1.403	N_{11B}–N_{12B}	1.403
N_9–N_{10}	1.389	N_1–N_2	1.402	N_5–N_6	1.390
N_{5E}–N_{6E}	1.389	N_{1E}–N_{2E}	1.390	N_{9B}–N_{10B}	1.402

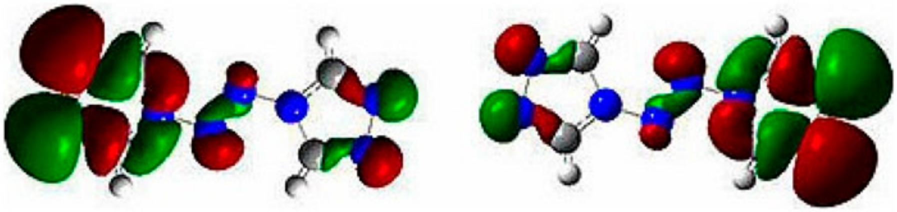

Figure 3. HOMO-1 and HOMO of atrz.

of N_9–Zn_1–N_{9A}, N_1–Zn_1–N_{1A}, N_{7B}–Zn_1–N_{7C}, N_9–Zn_1–N_1, N_1–Zn_1–N_{9A}, and N_{7C}–Zn_1–N_{9A} and the close bond lengths of Zn–N_9, Zn–N_1, and Zn–N_{7B} (shown in table 2). The length of azo double bond in the ligand is shorter than that (1.248 Å) in atrz due to the partly destroyed conjugated system by the central zinc. Every atrz in $\{[Zn(\mu\text{-atrz})_3](ClO_4)_2{\cdot}2H_2O\}_n$ serves as a bridging ligand connecting two zinc(II) ions to form a triangular-prism framework viewed down the *a*-axis (figure 6). The N_9 and N_{9A} ligands that might have enough freedom when they first came to the zinc cation are located in the same plane, but the other two pairs of ligands (N_1–N_{1A} and N_{7B}–N_{7C}) influenced by the former N_9 and N_{9A} ligands are bent to various degrees. The reaction sequence between N_1–N_{1A}, N_{7B}–N_{7C} ligands and zinc(II) can also be determined according to the length of N–Zn bonds [N_{7B}–Zn_1 (2.153 Å), N_1–Zn_1 (2.161 Å)]. That means a lot to the theoretical research of the

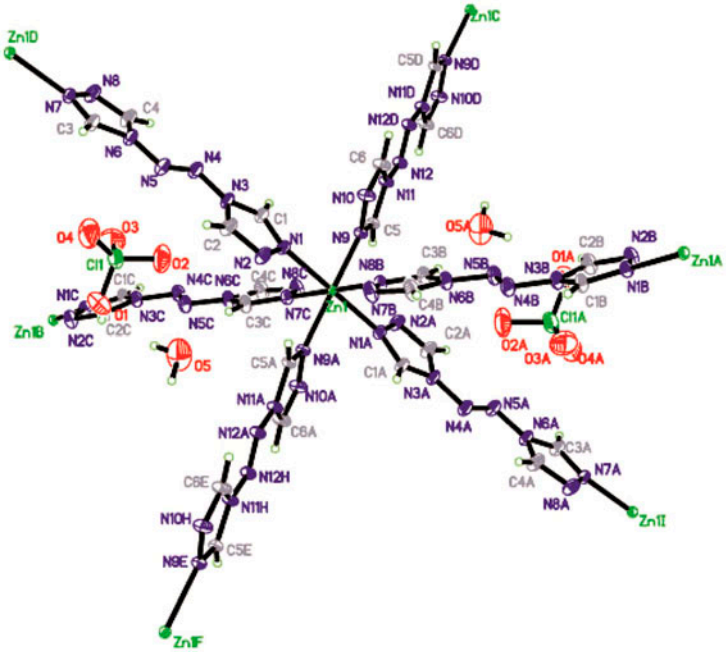

Figure 4. Coordination environment of the zinc cation in $\{[Zn(\mu\text{-atrz})_3](ClO_4)_2{\cdot}2H_2O\}_n$. Ellipsoids are drawn at 50% probability.

reaction mechanism between atrz and metal cations and the structural design of this kind of coordination compound. $\{[Cu(\mu\text{-atrz})_3](NO_3)_2{\cdot}2H_2O\}_n$ also crystallizes in the monoclinic space group *P2(1)/n* but a density of 1.683 g cm^{-3}, which is bigger than that of copper(II) thiocyanate complexes of 2-(2-pyridinyl)-benzthiazole, was synthesized by Chowdhury [44]. As shown in figure 5, the copper(II) is coordinated by six μ-atrz ligands in a nearly regular CuN_6 octahedron similar to ZnN_6, but ZnN_6 octahedron is more regular than that of CuN_6 because of the closer bond length of Zn–N_9, Zn–N_1, Zn–N_{7B} (shown in table 2). The bond length (1.403 Å) of N_{3E}–N_{4E} in $\{[Cu(\mu\text{-atrz})_3](NO_3)_2{\cdot}2H_2O\}_n$ is longer than that of N_5–N_6 in $\{[Zn(\mu\text{-atrz})_3](ClO_4)_2{\cdot}2H_2O\}_n$. Every two copper(II) ions are linked by atrz to form a triangular-prism framework viewed down the *a*-axis as for $\{[Zn(\mu\text{-atrz})_3](ClO_4)_2{\cdot}2H_2O\}_n$ displayed in figure 6. The reaction sequence between six ligands and copper(II) is N_9 and N_{9A}, N_{7B} and N_{7C}, and N_1 and N_{1A}. The length of azo double bond in $\{[Cu(\mu\text{-atrz})_3](NO_3)_2{\cdot}2H_2O\}_n$ is shorter than that in $\{[Zn(\mu\text{-atrz})_3](ClO_4)_2{\cdot}2H_2O\}_n$, because of the smaller ionic radius of copper(II).

3.3. *Theoretical explanation of the formation of $\{[Zn(\mu\text{-atrz})_3](ClO_4)_2{\cdot}2H_2O\}_n$ and $\{[Cu(\mu\text{-atrz})_3](NO_3)_2{\cdot}2H_2O\}_n$*

It is obvious that N_1 and N_8 (shown in figure S3) are the best coordination positions on the basis of natural charges (table S1) and the biggest green zone of HOMO (highest occupied molecular orbital) and HOMO-1 that are degenerated as shown in figure 3 because atrz is the electron donor. Generally, zinc(II) takes sp^3 hybridization to form four hybrid orbitals with 109° angle. Regular tetrahedral coordination structures exist in complexes of zinc(II).

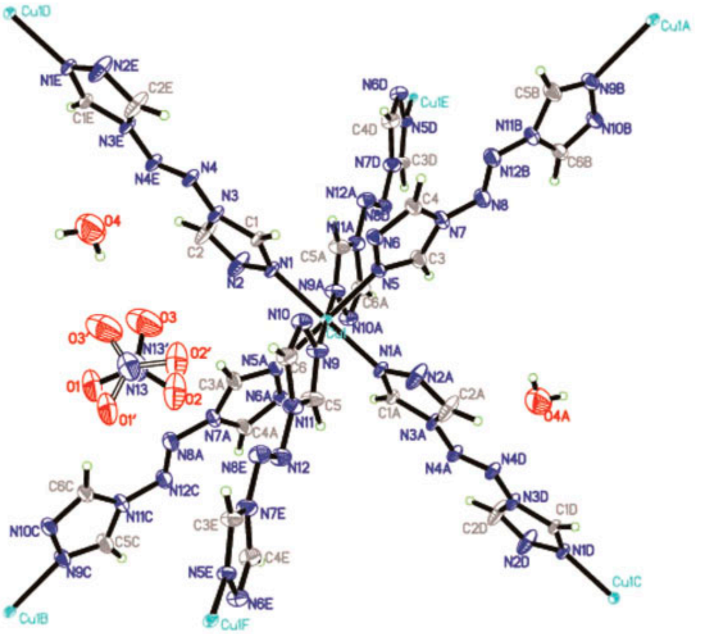

Figure 5. Coordination environment of copper(II) in$\{[Cu(\mu\text{-atrz})_3](NO_3)_2{\cdot}2H_2O\}_n$. Ellipsoids are drawn at 50% probability.

That is the same to copper(II). However, hybridization of sp^3d^2, higher energy and unstable, is taken by zinc(II) and copper(II) in $\{[Zn(\mu\text{-atrz})_3](ClO_4)_2{\cdot}2H_2O\}_n$ and $\{[Cu(\mu\text{-atrz})_3](NO_3)_2{\cdot}2H_2O\}_n$ in octahedral geometry. Some ligands are even bent (figure 7) to form the framework shown in figure 6. It is well known that three prism is more stable than four prism. The framework in $\{[Zn(\mu\text{-atrz})_3](ClO_4)_2{\cdot}2H_2O\}_n$ and $\{[Cu(\mu\text{-atrz})_3](NO_3)_2{\cdot}2H_2O\}_n$ is ideal and more stable despite the unstable sp^3d^2 hybridization and the bent ligands. Obviously, the formation of triangular prism framework leads to the formation of $\{[Zn(\mu\text{-atrz})_3](ClO_4)_2{\cdot}2H_2O\}_n$ and $\{[Cu(\mu\text{-atrz})_3](NO_3)_2{\cdot}2H_2O\}_n$.

3.4. *Relationship between structure and thermal property*

The typical DSC thermograms of atrz, $\{[Zn(\mu\text{-atrz})_3](ClO_4)_2{\cdot}2H_2O\}_n$ and $\{[Cu(\mu\text{-atrz})_3](NO_3)_2{\cdot}2H_2O\}_n$ are shown in figure 8. Two exothermic peaks of atrz were observed at 285.2 and 313.9 °C. As shown in table 2, the N_3–N_2 bond length (1.380 Å) is very close to that of N_{16}–N_1 (1.412 Å) and they are the two longest bonds in atrz. Therefore, breaking of N_3–N_2 and N_{16}–N_1 might lead to two exothermic peaks of atrz. In addition, breaking N_3–N_2 is easier than that of N_{16}–N_1 because of the stability of a five-membered ring despite the shorter bond length. However, the exothermic peaks of $\{[Zn(\mu\text{-atrz})_3](ClO_4)_2{\cdot}2H_2O\}_n$ are at 271.4 and 415.6 °C. The partly destroyed conjugated system makes the five-membered ring more stable but N_3–N_2 more unstable. So, the temperature difference of the exothermic peaks of $\{[Zn(\mu\text{-atrz})_3](ClO_4)_2{\cdot}2H_2O\}_n$ is bigger than that of atrz. The most stable crystal structure of $\{[Zn(\mu\text{-atrz})_3](ClO_4)_2{\cdot}2H_2O\}_n$ supplies the extra stability. So, their decomposition temperature is very close ($\{[Zn(\mu\text{-atrz})_3](ClO_4)_2{\cdot}2H_2O\}_n$ decomposes at

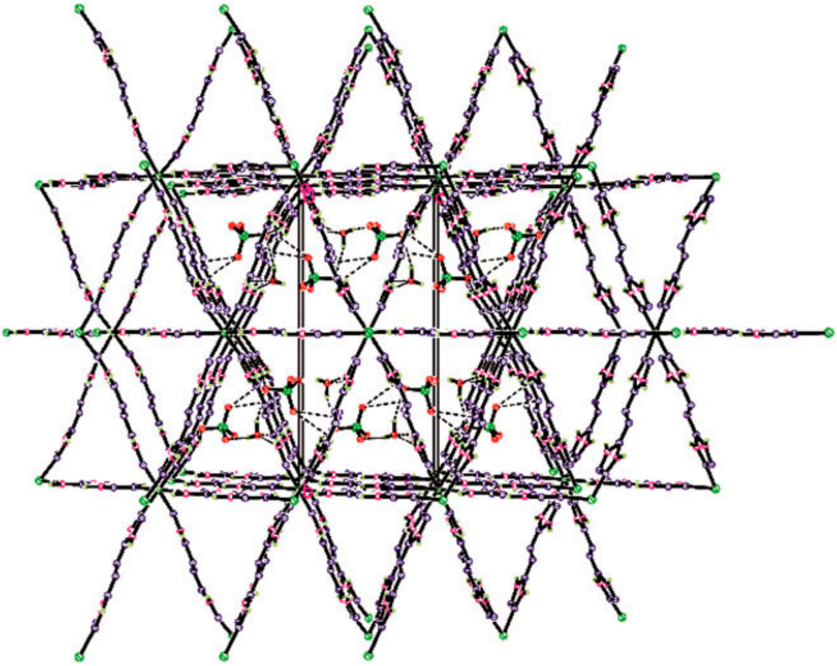

Figure 6. Part of the packing of $\{[Zn(\mu\text{-atrz})_3](ClO_4)_2\cdot 2H_2O\}_n$, viewed down the *a* direction. Dashed lines indicate hydrogen bonds.

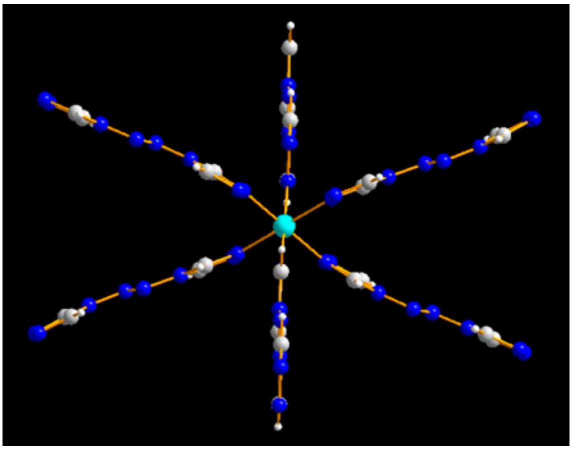

Figure 7. The bent ligand.

263.4 °C and atrz does at 268.4 °C). $\{[Cu(\mu\text{-atrz})_3](NO_3)_2\cdot 2H_2O\}_n$ with the same ligands and framework to $\{[Zn(\mu\text{-atrz})_3](ClO_4)_2\cdot 2H_2O\}_n$ decomposes at 223.9 °C and the second exothermic peak is at 368.3 °C, caused by the better thermal catalytic effect of cupric nitrate. The decomposition temperature of $\{[Zn(\mu\text{-atrz})_3](ClO_4)_2\cdot 2H_2O\}_n$ and $\{[Cu(\mu\text{-atrz})_3](NO_3)_2\cdot 2H_2O\}_n$ are lower than that of 3,6-bis (1H-1,2,3,4-tetrazol-5-ylamino)-1,2,4,5-tetrazine-based energetic strontium(II) complexes [45] and $[Cd(IMI)_2(N_3)_2]_n$ [46]. However,

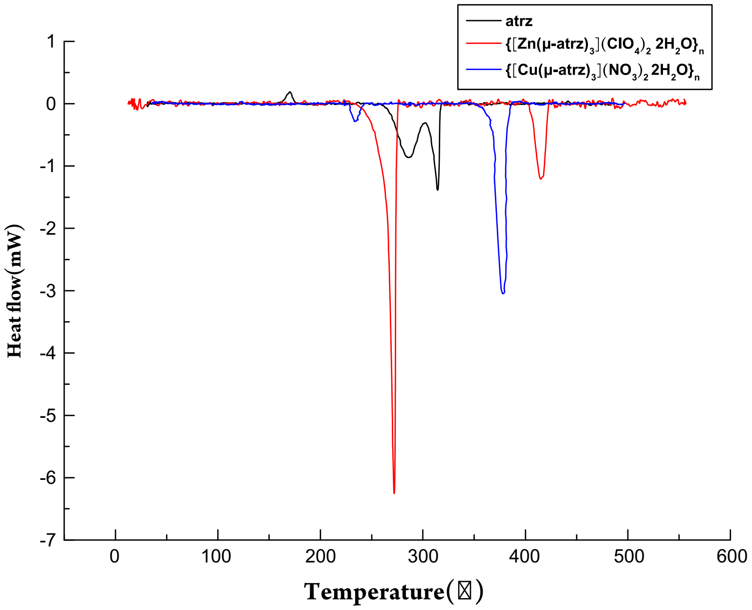

Figure 8. DSC thermogram of atrz, $\{[Zn(\mu\text{-atrz})_3](ClO_4)_2{\cdot}2H_2O\}_n$ and $\{[Cu(\mu\text{-atrz})_3](NO_3)_2{\cdot}2H_2O\}_n$.

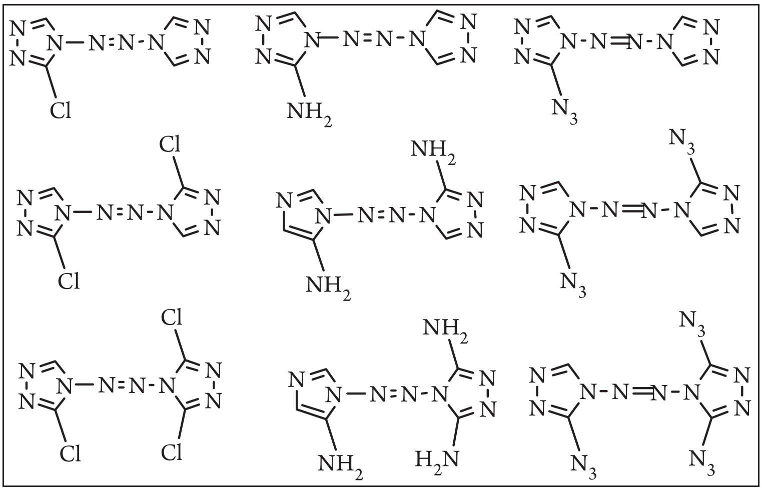

Figure 9. Some reported derivatives of atrz.

the same framework of $\{[Zn(\mu\text{-atrz})_3](ClO_4)_2{\cdot}2H_2O\}_n$ and $\{[Cu(\mu\text{-atrz})_3](NO_3)_2{\cdot}2H_2O\}_n$ gives them the same mechanical sensitivity (shown in table S2). $\{[Zn(\mu\text{-atrz})_3](ClO_4)_2{\cdot}2H_2O\}_n$ has a calculated statistical thermodynamics enthalpy of +1189.3 kJ M^{-1} at 298.15 K. Its high energy not only comes from ligands but the hybridization of sp^3d^2 of zinc(II) and potential energy of the bent ligands. $\{[Cu(\mu\text{-atrz})_3](NO_3)_2{\cdot}2H_2O\}_n$ gets higher statistical thermodynamics enthalpy of +1364.5 kJ M^{-1} at 298.15 K because of the more energy provided by cupric nitrate.

4. Conclusion

An improved synthetic pathway for atrz was developed. The pure atrz was obtained directly without separation step in an environment friendly process. The mode and position of coordination were confirmed using NBO analysis of atrz. The energetic materials composed of CPs, $\{[Zn(\mu\text{-atrz})_3](ClO_4)_2 \cdot 2H_2O\}_n$ and $\{[Cu(\mu\text{-atrz})_3](NO_3)_2 \cdot 2H_2O\}_n$ possessing both high energy and thermal stability, were synthesized using atrz as the ligand. The partly destroyed conjugation of ligands leads to different thermal behaviors of $\{[Zn(\mu\text{-atrz})_3](ClO_4)_2 \cdot 2H_2O\}_n$, $\{[Cu(\mu\text{-atrz})_3](NO_3)_2 \cdot 2H_2O\}_n$, and atrz. The better thermal catalytic effect of cupric nitrate makes $\{[Cu(\mu\text{-atrz})_3](NO_3)_2 \cdot 2H_2O\}_n$ to decompose at lower temperature. However, the crystal structure gives both high energy and thermal stability to $\{[Zn(\mu\text{-atrz})_3](ClO_4)_2 \cdot 2H_2O\}_n$ and $\{[Cu(\mu\text{-atrz})_3](NO_3)_2 \cdot 2H_2O\}_n$. The different properties between zinc perchlorate and cupric nitrate give the different thermal and energetic properties to $\{[Zn(\mu\text{-atrz})_3](ClO_4)_2 \cdot 2H_2O\}_n$ and $\{[Cu(\mu\text{-atrz})_3](NO_3)_2 \cdot 2H_2O\}_n$. Some derivatives of atrz (figure 9) have been reported. So, the ideal crystal structure and enormous possibilities of the introduction of high-nitrogen groups let us believe that the higher-nitrogen content energetic material will be produced soon. We believe that this new kind of energetic material will be an important member in the energetic materials family.

Acknowledgements

The authors are indebted to and thank State Key Laboratory of Explosion Science and Technology [grant number QNKT12-02], [grant number ZDKT10–01b] and Science and Technology on Applied Physical Chemistry Laboratory [grant number 9140C370303120C37142] of Beijing Institute of Technology for its financial support of this work. We thank the reviewers for their most valuable comments.

References

[1] S. Ritter. *Chem. Eng. News*, **82**, 44 (2004).
[2] F.R. Benson. *The High-Nitrogen Compounds*, Wiley-Interscience, New York (1984).
[3] D.E. Chavez, M.A. Hiskey, R.D. Gilardi. *Angew. Chem. Int. Ed.*, **39**, 1791 (2000).
[4] J. Kerth, S. Lobbecke. *Propellants, Explos., Pyrotech.*, **27**, 111 (2002).
[5] M.H.V. Huynh, M.A. Hiskey, E.L. Hartline, D.P. Montoya, R.D. Gilardi. *Angew. Chem. Int. Ed.*, **43**, 4924 (2004).
[6] G. Zhou, J.L. Zhang, N.B. Wong, A. Tian. *J. Mol. Struct. Theochem.*, **668**, 189 (2004).
[7] J. Neutz, O. Grosshardt, S. Schaufele, H. Schuppler, W. Schweikert. *Propellants, Explos., Pyrotech.*, **28**, 181 (2003).
[8] M.H.V. Huynh, M.A. Hiskey, C.J. Pollard, D.P. Montoya, E.L. Hartline, R.D. Gilardi. *J. Energ. Mater.*, **22**, 217 (2004).
[9] A.M. Churakov, O.Y. Smirnov, S.L. Ioffe, Y.A. Strelenko, V.A. Tartakovsky. *Eur. J. Org. Chem.*, **14**, 2342 (2002).
[10] V.A. Tartakovsky. *Mater. Res. Soc. Sym. Proc.*, **418**, 15 (1996).
[11] A.N. Ali, S.F. Son, M.A. Hiskey, D.L. Naud. *J. Propul. Power*, **20**, 120 (2004).
[12] S.F. Son, H.L. Berghout, C.A. Bolme, D.E. Chavez, D.L. Naud, M.A. Hiskey. *Proc. Combust. Inst.*, **28**, 919 (2000).
[13] H.S. Jadhav, D.D. Dhavale, V.N. Krishnamurthy. *Theory Pract. Energ. Mater.*, **4**, 493 (2001).
[14] D.E. Chavez, M.A. Hiskey, D.L. Naud. *J. Pyrotech.*, **10**, 17 (1999).
[15] D.E. Chavez, M.A. Hiskey. *J. Pyrotech.*, **7**, 11 (1998).
[16] M.H.V. Huynh, M.A. Hiskey, D.E. Chavez, D.L. Naud, R.D. Gilardi. *J. Am. Chem. Soc.*, **127**, 12537 (2005).

[17] A. Hammerl, M.A. Hiskey, G. Holl, T.M. Klapötke, K. Polborn, J. Stierstorfer, J.J. Weigand. *Chem. Mater.*, **17**, 3784 (2005).

[18] D.E. Chavez, M.A. Hiskey. *J. Heterocycl. Chem.*, **35**, 1329 (1998).

[19] D.E. Chavez, M.A. Hiskey, R.D. Gilardi. *Org. Lett.*, **6**, 2889 (2004).

[20] T.M. Klapötke, D.G. Piercey. *Inorg. Chem.*, **50**, 2732 (2011).

[21] T.M. Klapötke, P. Mayer, A. Schulz, J.J. Weigand. *J. Am. Chem. Soc.*, **127**, 2032 (2005).

[22] M. Göbel, K. Karaghiosoff, T.M. Klapötke, D.G. Piercey, J. Stierstorfer. *J. Am. Chem. Soc.*, **132**, 17216 (2010).

[23] T.M. Klapötke, C. Kuffer, P. Mayer, K. Polborn, A. Schulz, J.J. Weigand. *Inorg. Chem.*, **44**, 5949 (2005).

[24] J. Heppekausen, T.M. Klapötke, S.M. Sproll. *J. Org. Chem.*, **74**, 2460 (2009).

[25] V. Thottempudi, H.-X. Gao, J.M. Shreeve. *J. Am. Chem. Soc.*, **133**, 6464 (2011).

[26] V. Thottempudi, J. Shreeve. *J. Am. Chem. Soc.*, **133**, 19982 (2011).

[27] Y.-C. Li, C. Qi, S.-H. Li, H.-J. Zhang, C.-H. Sun, Y.-Z. Yu, S.-P. Pang. *J. Am. Chem. Soc.*, **132**, 12172 (2010).

[28] S.-H. Li, S.-P. Pang, X.-T. Li, Y.-Z. Yu, X.-Q. Zhao. *Chin. Chem. Lett.*, **18**, 1176 (2007).

[29] C. Qi, S.-H. Li, Y.-C. Li, Y. Wang, X.-K. Chen, S.-P. Pang. *J. Mater. Chem.*, **21**, 3221 (2011).

[30] S.-H. Li, H.-G. Shi, C.-H. Sun, X.-T. Li, S.-P. Pang, Y.-Z. Yu, X.-Q. Zhao. *J. Chem. Crystallogr.*, **39**, 13 (2009).

[31] C. Qi, S.-H. Li, Y.-C. Li, Y. Wang, X.-X. Zhao, S.-P. Pang. *Chem. Eur. J.*, **18**, 16562 (2012).

[32] Y. Fujiwara, J.A. Dixon, F.O. Hara, E.D. Funder, D.D. Dixon, R.A. Rodriguez, R.D. Baxter, B. Herlé, N. Sach, M.R. Collins, Y. Ishihaha, P.S. Baran. *Nature*, **492**, 95 (2012).

[33] X.-M. Liu, B.-Y. Wang, W. Xue, L.-H. Xie, W.-X. Zhang, X.-N. Cheng, X.-M. Chen. *Dalton Trans.*, 13741 (2012).

[34] Y.-C. Chuang, C.-T. Liu, C.-F. Sheu, W.-L. Ho, G.-H. Lee, C.-C. Wang, Yu. Wang. *Inorg. Chem.*, **51**, 4663 (2012).

[35] G.M. Sheldrick. *Program for the Solution of Crystal Structures, SHELXS-97*, University of Göttingen, Germany (1997).

[36] G.M. Sheldrick. *Program for Crystal Structure Refinement from Diffraction Data, SHELXS-97*, University of Göttingen, Germany (1997).

[37] M.J. Frisch, G.W. Trucks, H.B. Schlegel, G.E. Scuseria, M.A. Robb, J.R. Cheeseman, J.A. Montgomery, J.T. Vreven, K.N. Kudin, J.C. Burant, J.M. Millam, S.S. Iyengar, J. Tomasi, V. Barone, B. Mennucci, M. Cossi, G. Scalmani, N. Rega, G.A. Petersson, H. Nakatsuji, M. Hada, M. Ehara, K. Toyota, R. Fukuda, J. Hasegawa, M. Ishida, T. Nakajima, Y. Honda, O. Kitao, H. Nakai, M. Klene, X. Li, J.E. Knox, H.P. Hratchian, J.B. Cross, C. Adamo, J. Jaramillo, R. Gomperts, R.E. Stratmann, O. Yazyev, A.J. Austin, R. Cammi, C. Pomelli, J.W. Ochterski, P.Y. Ayala, K. Morokuma, G.A. Voth, P. Salvador, J.J. Dannenberg, V.G. Zakrzewski, S. Dapprich, A.D. Daniels, M.C. Strain, O. Farkas, D.K. Malick, A.D. Rabuck, K. Raghavachari, J.B. Foresman, J.V. Ortiz, Q. Cui, A.G. Baboul, S. Clifford, J. Cioslowski, B.B. Stefanov, G. Liu, A. Liashenko, P. Piskorz, I. Komaromi, R.L. Martin, D.J. Fox, T. Keith, M.A. Al-Laham, C.Y. Peng, A. Nanayakkara, M. Challacombe, P.M.W. Gill, B. Johnson, W. Chen, M.W. Wong, C. Gonzalez, J.A. Pople. *Gaussian 03 (Revision C.03)*, Gaussian Inc., Pittsburgh, PA (2003).

[38] B. Delley. *J. Chem. Phys.*, **92**, 508 (1990).

[39] B. Delley. *J. Chem. Phys.*, **113**, 7756 (2000).

[40] J.P. Perdew, Y. Wang. *Phys. Rev. B*, **45**, 13244 (1992).

[41] M. Dolg, U. Wedig, H. Stoll, H. Preuss. *J. Chem. Phys.*, **86**, 866 (1987).

[42] A. Bergner, M. Dolg, W. Kuchle, H. Stoll, H. Preuss. *Mol. Phys.*, **80**, 1431 (1993).

[43] Z.-M. Li, T.-L. Zhang, G.-T. Zhang, Z.-N. Zhou, L. Yang, J.-G. Zhang, K.-B. Yu. *J. Coord. Chem.*, **66**, 1276 (2013).

[44] S. Chowdhury, S. Majumder, A. Bhattacharya, P. Mitra, J.P. Naskar. *J. Coord. Chem.*, **66**, 3365 (2013).

[45] X.-B. Zhang, Y.-H. Ren, W. Li, F.-Q. Zhao, J.-H. Yi, B.-Z. Wang, J.-R. Song. *J. Coord. Chem.*, **66**, 2051 (2013).

[46] B.-D. Wu, Y.-G. Bi, Z.-N. Zhou, L. Yang, J.-G. Zhang, T.-L. Zhang. *J. Coord. Chem.*, **66**, 3014 (2013).